Medical Dosimetry 38 (2013) 337–343

Medical Dosimetry

journal homepage: www.meddos.org

The effect of the target-organ geometric complexity on the choice of delivery between RapidArc and sliding-window IMRT for nasopharyngeal carcinoma

Monica W.K. Kan, M.Phil.,*† Lucullus H.T. Leung, Ph.D.,* and Peter K.N. Yu, Ph.D.†

*Department of Oncology, Princess Margaret Hospital, Hong Kong SAR, People's Republic of China; and †Department of Physics and Materials Science, City University of Hong Kong, Kowloon Tong, Hong Kong SAR, People's Republic of China

ARTICLE INFO

Article history:
Received 22 February 2012
Accepted 8 March 2013

Keywords:
Nasopharyngeal carcinoma
RapidArc
IMRT
Target-organ complexity
Anatomic features

ABSTRACT

We attempted to assess the effect of target-organ geometric complexity on the plan quality of sliding-window intensity-modulated radiotherapy (IMRT), double-arc (RA2), and triple-arc (RA3) RapidArc volumetric-modulated arc radiotherapy for nasopharyngeal carcinoma (NPC). Plans for 9-field sliding-window IMRT, RA2, and RA3 were optimized for 36 patients with NPC ranging from T1 to T4 tumors. Initially the patients were divided into 2 groups, with group A representing the most simple early stage (T1 and T2) cases, whereas group B represented the more complex advanced cases (T3 and T4). Evaluation was performed based on target conformity, target dose homogeneity, organ-sparing capability, and delivery efficiency. Based on the plan quality results, a subgroup of advanced cases, group B2, representing the most demanding task was distinguished and reported separately from the rest of the group B cases, B1. Detailed analysis was performed on the anatomic features for each group of cases, so that planners can easily identify the differences between B1 and B2. For the group A cases, RA3 plans were superior to the IMRT plans in terms of organ sparing, whereas target conformity and dose homogeneity were similar. For the group B1 cases, the RA3 plans produced almost equivalent plan quality as the IMRT plans. For the group B2 cases, for most of which large target volumes were adjacent to (5 mm or less) and wrapping around the brain stem, RA2 and RA3 were inferior to the IMRT regarding both target dose homogeneity and conformity. RA2 plans were slightly inferior to IMRT and RA3 plans for most cases. The plan comparison results depend on the target to brain stem distances and the target sizes. The plan quality results together with the anatomic information may allow the evaluation of the 3 treatment options before actual planning.

Introduction

Recently, volumetric-modulated arc therapy (VMAT) has attracted significant attention owing to its capability of providing highly conformal dose distribution with good delivery efficiency. It is an arc-based approach of intensity-modulated radiotherapy (IMRT) that allows irradiation with simultaneously changing multileaf collimator (MLC) position, gantry position, and dose rate.[1,2] Various treatment planning studies have been published showing that it is more efficient than conventional static IMRT.[3-13]

Many investigations were done on planning comparison between VMAT and conventional IMRT in head and neck cases.[6-13] The cases chosen by previous authors mostly involved a mixture of various sites including the nasopharynx, oropharynx, larynx, and hypopharynx. As the location of the nasopharyngeal region is at a more superior level compared with other head and neck cases, and the target volumes are surrounded by a relatively larger volume of critical organs, including brain stem, spinal cord, parotid glands, and optical structures. It is better if the assessment for cases of nasopharyngeal carcinoma (NPC) cases is separated from other head and neck sites.

Although dosimetric evaluation on the use of VMAT for purely NPC cases was done by a few authors,[10,12,13] the effect of target-organ complexity on plan quality for different delivery techniques has not been studied. In our study, plan evaluation of RapidArc (RA, Varian Medical Systems, Palo Alto, CA) compared with sliding-window IMRT (sw-IMRT) for early stage patients (T1 and T2), group A, were separated from that of advanced stage patients (T3 and T4), group B. As previous studies proved that the use of single-arc VMAT provides inferior or unacceptable plan quality than double-arc VMAT in head and neck cases,[6-13] the use of

Reprint requests to: Monica W.K. Kan, M.Phil., Department of Oncology, Princess Margaret Hospital, Hong Kong SAR, People's Republic of China. Tel.: +852 2990-2776; fax: +852 2990-2775.
E-mail: kanwkm@ha.org.hk

0958-3947/$ – see front matter
http://dx.doi.org/10.1016/j.meddos.2013.03.006

single-arc VMAT was excluded from this study. Only double-arc and triple-arc plans were evaluated.

It was found that the plan comparison results for advanced stage patients were mixed. RA using even 3 arcs produced inferior plan quality for a subgroup of advanced cases compared with sw-IMRT, whereas quite equivalent plan quality could be achieved for the remaining cases with modest complexity. The authors reported the plan evaluation results of the most difficult cases, that is the subgroup B2, separately from the rest of the advanced cases, group B1. Detailed anatomic analysis were performed on the 3 groups of patients, A, B1, and B2, to discern the anatomic features of group B2 from B1 and A. This might help determine the choice of delivery for NPC cases with different complexity levels.

Methods and Materials

Patient selection and contouring

Double-arc RA (RA2), triple-arc RA (RA3), and 9-field sw-IMRT plans were created for 36 patients with NPC, ranging from Stage I to IV tumors (1997 International Union Against Cancer/American Joint Committee on Cancer stage classification). All the plans were generated using the Eclipse version 8.6 (Varian Medical Systems Inc, Palo Alto, CA). Cases 1 through 14 represented relatively simple and early stage (Stage I and II only) cases and were categorized as group A cases. Cases 15 to 36 were advanced and complex cases (Stage III or IV) and were categorized as group B cases.

The primary gross tumor volume (GTV_{70}) covered the gross tumor plus the entire nasopharynx down to caudal border of C1 vertebra. The nodal gross tumor volume (GTV_{N70}) encompassed any positive lymph nodes as defined by a short axis of greater than 1 cm. The boost clinical target volume (CTV_{70}) and the nodal clinical target volume (CTV_{N70}) were formed by adding 0.5-cm margin to GTV_{70} and GTV_{N70}, respectively. The high-risk clinical target volume (CTV_{60}) was created by adding 1-cm margin to CTV_{70} and CTV_{N70} plus minimal coverage for high-risk elective sites including lower half of sphenoid sinus, anterior half of clivus, base of skull, petrous tips, posterior third of nasal cavity and maxillary sinuses, pterygoid fossae, parapharyngeal spaces, and lymph nodes bilaterally. The low-risk clinical target volume (CTV_{54}) covered bilateral level IV and Vb nodal regions unless positive lymph nodes were present where CTV_{60} would extend into level IV and Vb to 0.15 cm below caudal border of CTV_{N70}. The boost planning target volume with nodal planning target volume (PTV_{70}), high-risk planning target volume (PTV_{60}), and low-risk planning target volume (PTV_{54}) were produced by adding 0.3 cm to CTV_{70} with CTV_{N70}, CTV_{60}, and CTV_{54}, respectively. The prescriptions were as follows: 70 Gy was given to the PTV_{70}, 60 Gy was given to PTV_{60}, and 54 Gy was given to the PTV_{54}. The International Commission on Radiation Units and Measurements (ICRU) specifies that the heterogeneity in dose delivery to the PTV should be kept within 95 to 107%.[14,15] Our goal was to give at least 95% of the PTV and 100% of the GTV the prescribed dose, the PTV_{70} would receive no more than 107% of the prescribed dose. The dose constraints to organs at risk are summarized in Table 1.

IMRT planning

The IMRT plans were created using 9-field sliding-window technique with all fields distributed evenly in coplanar beam directions. All beam energies were 6 MV and modulated with 120 MLC from a linear accelerator (Clinac 6EX, Varian Medical Systems). Optimizations and dose calculations were done with Eclipse version 8.6.15. The optimization dose priorities were similar for all cases. Giving enough dose coverage to PTVs and limiting the maximum doses to brain stem, spinal cord, optic nerves, and optic chiasma were given the highest priority, followed by reducing the dose to parotid glands. Lower priorities were given to the other critical organs. An optimization criteria was also assigned to an organ representing normal tissues, which was defined as the body volume in the computed tomography data set minus the PTV leaving 3-mm gap. Dose calculation was performed with Analytical Anisotropic Algorithm using a calculation grid of 2.5 mm. All IMRT plans were high-quality plans generated by experienced planners following the institutional planning conventions.

RA planning

Optimization with version 8.6.15 allows the use of multiple arc fields, nonzero couch angles, and avoidance sectors. A plan can be created using a maximum of 10 arc fields with a maximum total arc length of 1000°. The final dose calculation is performed in Eclipse by the Analytical Anisotropic Algorithm.

For RA2, 2 complete arcs, 1 moving clockwise from 181° to 179° and the other moving anticlockwise from 179° to 181° were used. The RA3 plans were created using 2 complete arcs plus 1 partial arc, *i.e.* 2 complete arcs with gantry rotation the same as in the RA2 with an additional arc ranging from 220° to 140° in the clockwise direction.

Nonzero collimator angles were used to reduce the tongue-and-groove effect. In this study, a collimator angle range from 30° to 45° was used for the first arc, 320° to 345° for the second arc, and 5° to 20° for the third arc. The optimization aims were the same as those for sw-IMRT plans. However, the optimization template was different from that of sw-IMRT due to the differences in optimization algorithm between the 2 techniques. The same initial optimization template was used in RA2 and RA3 plans for all patients. Optimizations were repeated 5 to 6 times to improve the plan quality depending on the complexity of the plan. To reduce the bias due to operator skill, all the plans were generated by one single planner and reviewed by an experienced physicist.

Table 1
The dose constraints to organs at risk

Organs at risk	Maximum (given the first priority if achievable) (Gy)	Dose volume constraints (Gy)
Brain stem	54	
Brain stem + 3 mm		≤ 1 mL or 1% to receive up to 60 Gy*
Spinal cord	45	
Spinal cord + 5 mm		≤ 1 mL or 1% to receive up to 50 Gy*
Optic nerves/chiasm	54	≤ 1% to receive up to 60 Gy*
Temporal lobes	60	< 1% to exceed 65 Gy*
Parotid glands		mean dose ≤ 26 Gy (given the first priority if achievable) or < 50% to exceed 30 Gy*
Eyes	45	Mean dose < 35 Gy*
Ears	58	Mean dose < 50 Gy*
Lens	6	Mean dose < 10 Gy*
Pituitary	45	< 1% to exceed 65 Gy*
Brachial plexus	63	

* The dose volume constraints that must be achieved if the maximum dose is exceeded.

Plan evaluation

The plan conformity was evaluated using the conformation number (CN) that was defined as the product of $V_{T,\,ref}/V_T$ and $V_{T,\,ref}/V_{ref}$, where $V_{T,\,ref}$ represents the volume of the target receiving a dose equal to or greater than the reference dose; V_T represents the physical volume of the target, and V_{ref} represents the total tissue volume receiving a dose equal to or greater than the reference dose.[16] The reference dose used to compute the CN is the prescription dose. The first fraction assesses quality of target coverage, and the second fraction assesses the amount of healthy tissue being involved in the reference dose. The higher the CN values, the better the conformity. A CN value of 1 represents perfect conformity.

The uniformity index was used to describe the target dose homogeneity of the plans,[17] which was defined as:

$$UI = \frac{D_{5\%}}{D_{95\%}}, \quad (1)$$

where UI is the uniformity index and $D_{5\%}$ and $D_{95\%}$ are the minimum doses delivered to 5% and 95% of the PTV. A higher UI indicates higher target dose heterogeneity. Besides, for all the plans, the coverage represented by $V_{>\ 100\%}$ (the volume receiving more than 100% of the reference dose), $V_{>\ 95\%}$ and the hot areas represented by $V_{>\ 107\%}$ were reported for PTV_{70}.

For the organ at risk (OAR), the volume of parotid glands receiving more than 30 Gy ($V_{30\ Gy}$), the dose encompassing 1% ($D_{1\%}$) of the volume for brain stem, spinal cord, optic chiasm, optic nerve, and the mean doses to lens were also reported. The Wilcoxon matched-pair signed rank test was used to test the significance of the results.

Distinguishing a subgroup from the advanced NPC cases

It was found from the plan evaluation results that the target dose (PTV_{70}) homogeneity of a subgroup of advanced cases (cases 25 to 36) did not satisfy the ICRU acceptable range of 95% to 107% for all RA plans even when 3 arcs were used. The 95% coverage was properly achieved by all plans, but significantly more hot areas were found in this subgroup using RA2 and RA3. The distribution of $V_{>107\%}$ and the UI values for all 36 patients were shown in Figs. 1 and 2, respectively. These cases were assigned to a subgroup, B2. The conformity and organ sparing of B2 were also slightly inferior using RA compared with sw-IMRT. Initial observation of

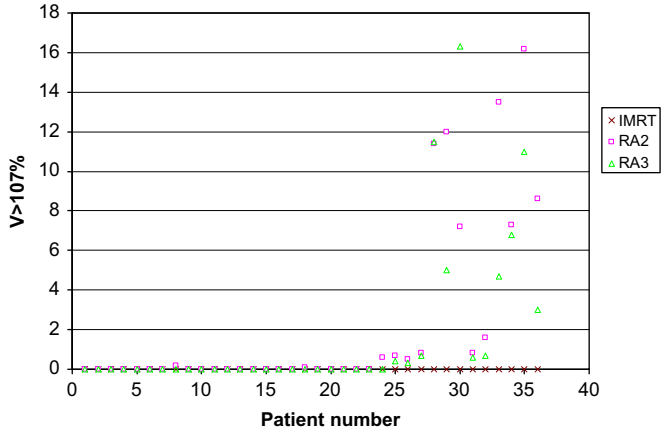

Fig. 1. Distribution of the $V_{>70\%}$ of PTV_{70} for the 36 patients with NPC. (Color version of figure is available online.)

this subgroup were a mixture of T3 and T4 cases with relatively more concave large target volumes. The dependence of plan quality on patient geometry was investigated by a few authors.[18,19] It is believed that the plan quality mainly depends on the complexity of patient geometry.

Anatomic analysis

To identify those patient features that might distinguish B2 from the rest of the cases, different anatomic features were collected for the 36 patients. The selection was based on our clinical experience. The features included were listed in Table 4. They described the proximity of the brain stem, spinal cord, optical structures, and parotids to the target volumes. The shortest distances between the brain stem and the target PTV_{70} were found by measuring the shortest distances between the 2 contours on each CT slice and then taking the average of the 3 smallest values. Similar procedures were performed between the brain stem and PTV_{60}, the spinal cord and PTV_{70}, the spinal cord and PTV_{60}, and skin and the nodal target volume. To get the relationship between the brain stem and PTVs in 3-dimensional space, the contour of the brain stem was expanded evenly in all directions by 1 cm, the overlapping volumes between the expanded brain stem and PTVs were reported. The same was performed for spinal cord. The percentage volume of parotid overlapping with PTV_{60} were found by calculating [(volume of $PTV_{60} \cap$ volume of parotid)/volume of parotid] $\times$ 100%). The reported values were the mean of left and right parotid. The longitudinal distance between the lens and the superior border of PTV_{60} represents the proximity of the optical structures to the target volume. It was found by measuring the longitudinal distances between the base of the lens and the most superior slice involving PTV_{60} on the sagittal view. The values of each anatomic feature were collected and reported separately for group A, B1, and B2. Statistical analysis were performed to see if there was any significant differences of the features between the couples, A and B1, A and B2, and B1 and B2. Statistical analysis was done using the analysis of variance test with the Tukey test when the data followed the normal distribution. Otherwise, the nonparametric Krukal-Wallis test was used followed by the Mann-Whitney U test.

Results

Plan quality for group A cases

Table 2 summarizes the results of PTV coverage, OAR doses, and plan evaluation indices averaged over the 14 early stage group A cases. All plans achieved satisfactory coverage for 95% of the reference dose to PTVs. There was no difference in CN and UI between RA3 and IMRT. The higher values of $V_{>100\%}$ produced by both RA2 and RA3 plans indicated slightly better coverage for PTV_{70} compared with sw-IMRT. The lowest CN and highest UI values indicated that RA2 produced inferior conformity and target dose homogeneity than the other 2 delivery methods.

RA3 was able to provide the best organ sparing. This was clearly reflected from lowest V_{30} Gy of the parotid glands and the $D_{1\%}$ of the spinal cord achieved by it. The V_{30} Gy of the parotid glands could be reduced from 37.7% to 31.6% using RA3 compared with IMRT. The V_{30} Gy of the parotid glands produced by RA2 was 42.4%, which was highest among the 3 techniques. The use of RA2 and RA3 plans slightly increased the mean doses to lens by 0.3 to 0.4 Gy, respectively, compared with IMRT. On the whole RA3 produced superior plan quality than both IMRT and RA2.

Plan quality for group B cases

Table 3 summarizes the plan evaluation results averaged for the advanced cases. For group B1 cases, there was no significant difference in CN and UI between IMRT and RA3, whereas RA2 produced both inferior target homogeneity and conformity than RA3. The use of RA3 for this group did not show any dosimetric benefit in OAR sparing as in group A. RA3 produced comparable doses to most critical organs as IMRT. RA2 produced inferior organ sparing compared with the other 2 methods. The V_{30} Gy of the

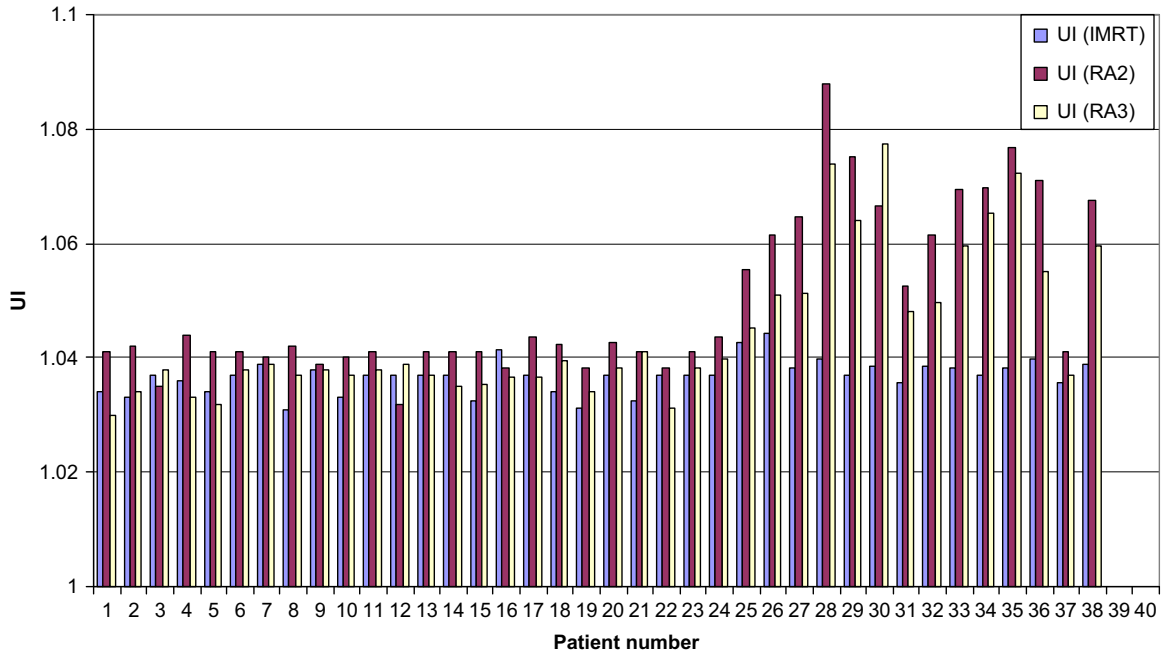

Fig. 2. Distribution of the UI values for the 36 early stage patients with NPC. (Color version of figure is available online.)

Table 2
Summary of the PTV coverage, OAR doses, plan evaluation indexes, and the overall plan quality scores averaged for the 14 early stage group A cases

	Static IMRT	Double-arc RA	Triple-arc RA	$p < 0.05$ x:IMRT *vs* RA3 y:IMRT *vs* RA2 z:RA3 *vs* RA2
$V_{>100\%}$ for PTV_{70}, %	97.5 ± 1.0	98.4 ± 0.8	98.9 ± 0.5	x, y
$V_{>95\%}$ for PTV_{70}, %	100.0 ± 0.02	100.0 ± 0.01	100.0 ± 0.01	–
$V_{>100\%}$ for PTV_{60}, %	98.7 ± 0.7	98.5 ± 0.7	98.5 ± 0.7	–
$V_{>95\%}$ for PTV_{60}, %	99.9 ± 0.1	99.9 ± 0.1	99.9 ± 0.1	–
$V_{>100\%}$ for PTV_{54}, %	98.7 ± 0.8	98.4 ± 0.8	98.8 ± 0.9	–
$V_{>95\%}$ for PTV_{54}, %	99.9 ± 0.1	99.8 ± 0.3	99.9 ± 0.2	–
$V_{>107\%}$ for PTV_{70}, %	0.00 ± 0.00	0.02 ± 0.04	0.00 ± 0.00	–
UI PTV_{70}	1.036 ± 0.002	1.040 ± 0.003	1.036 ± 0.003	y, z
CN PTV_{70}	0.87 ± 0.020	0.84 ± 0.027	0.86 ± 0.023	y, z
CN PTV_{60}	0.87 ± 0.020	0.87 ± 0.028	0.88 ± 0.017	–
Brain stem $D_{1\%}$, Gy	49.6 ± 1.6	50.3 ± 1.2	49.0 ± 1.3	z
Spinal cord $D_{1\%}$, Gy	40.9 ± 1.6	41.2 ± 1.2	40.1 ± 0.9	x, z
Optic chiasma $D_{1\%}$, Gy	16.5 ± 11.0	15.9 ± 9.2	15.4 ± 9.3	–
Optic nerve $D_{1\%}$, Gy	18.2 ± 11.7	16.5 ± 10.7	16.3 ± 10.0	–
Lens mean dose, Gy	3.9 ± 0.4	4.3 ± 0.5	4.2 ± 0.3	x, y
Parotid V_{30}, %	37.7 ± 8.7	42.4 ± 8.6	31.6 ± 7.0	x, y, z
Monitor units	1541 ± 231	704 ± 117	713 ± 97	x, y

parotid glands was 43.2%, which was the highest among the 3 techniques. RA2 and RA3 increased the mean doses to lens by about 1.3 Gy. The overall plan quality of RA3 was quite equivalent to that of IMRT.

For the group B2 cases, IMRT produced the highest CN and lowest UI among the 3 methods. Only IMRT could meet the ICRU standard of target dose homogeneity. Significantly more hot areas appear in RA plans. The averaged value of $V_{>107\%}$ was 0%, 6.7%, and

Table 3
Summary of the PTV coverage, OAR doses, plan evaluation indices, and the overall plan quality scores averaged for the 10 advanced stage group B1 and the most complex 12 advanced group B2 cases

	Static IMRT	Double-arc RA	Triple-arc RA	$p < 0.05$ x:IMRT *vs* RA3 y:IMRT *vs* RA2 z:RA3 *vs* RA2
		Group B1		
$V_{>100\%}$ for PTV_{70}, %	97.9 ± 1.1	98.0 ± 1.9	98.8 ± 0.8	x, z
$V_{>95\%}$ for PTV_{70}, %	100 ± 0.01	100 ± 0.02	100 ± 0.02	–
$V_{>100\%}$ for PTV_{60}, %	98.8 ± 0.5	98.4 ± 0.6	98.7 ± 0.4	z
$V_{>95\%}$ for PTV_{60}, %	100.0 ± 0.2	99.9 ± 0.3	99.9 ± 0.2	–
$V_{>100\%}$ for PTV_{54}, %	98.6 ± 1.1	97.3 ± 1.5	98.2 ± 1.0	y, z
$V_{>95\%}$ for PTV_{54}, %	99.9 ± 0.3	99.8 ± 0.4	99.9 ± 0.2	–
$V_{>107\%}$ for PTV_{70}, %	0.000 ± 0.000	0.073 ± 0.190	0.002 ± 0.004	y
UI PTV_{70}	1.036 ± 0.003	1.041 ± 0.002	1.037 ± 0.003	y, z
CN PTV_{70}	0.878 ± 0.020	0.865 ± 0.012	0.877 ± 0.010	z
CN PTV_{60}	0.871 ± 0.020	0.88 ± 0.013	0.89 ± 0.020	–
Brain stem $D_{1\%}$, Gy	49.1 ± 1.7	49.3 ± 1.9	49.2 ± 1.6	–
Spinal cord $D_{1\%}$, Gy	39.2 ± 1.4	40.5 ± 1.3	40.6 ± 1.8	–
Optic chiasma $D_{1\%}$, Gy	51.6 ± 6.0	52.0 ± 6.5	51.8 ± 6.7	–
Optic nerve $D_{1\%}$, Gy	51.1 ± 8.6	50.6 ± 8.5	50.7 ± 8.7	–
Lens mean dose, Gy	4.3 ± 0.7	5.6 ± 1.1	5.7 ± 1.0	x, y
Parotid V_{30}, cm^3	38.1 ± 13.9	43.2 ± 14.6	35.8 ± 13.8	y, z
Monitor units	1643 ± 174	668 ± 88	694 ± 105	x, y
		Group B2		
$V_{>100\%}$ for PTV_{70}, %	96.9 ± 0.6	96.1 ± 1.6	97.3 ± 1.1	z
$V_{>95\%}$ for PTV_{70}, %	99.9 ± 0.1	99.9 ± 0.2	99.9 ± 0.2	–
$V_{>100\%}$ for PTV_{60}, %	98.9 ± 0.4	98.2 ± 0.6	98.6 ± 0.4	y, z
$V_{>95\%}$ for PTV_{60}, %	100.0 ± 0.2	99.8 ± 0.4	99.9 ± 0.3	–
$V_{>100\%}$ for PTV_{54}, %	97.8 ± 2.1	97.2 ± 1.9	97.5 ± 1.9	–
$V_{>95\%}$ for PTV_{54}, %	99.9 ± 0.3	99.7 ± 0.5	99.8 ± 0.3	–
$V_{>107\%}$ for PTV_{70}, %	0.000 ± 0.000	6.72 ± 5.73	5.08 ± 5.33	x, y, z
UI PTV_{70}	1.039 ± 0.002	1.067 ± 0.010	1.059 ± 0.010	x, y, z
CN PTV_{70}	0.886 ± 0.018	0.863 ± 0.017	0.864 ± 0.021	x, y
CN PTV_{60}	0.877 ± 0.015	0.886 ± 0.013	0.885 ± 0.018	–
Brain stem $D_{1\%}$, Gy	52.2 ± 1.9	53.8 ± 1.8	53.4 ± 2.5	y
Spinal cord $D_{1\%}$, Gy	40.8 ± 1.4	40.5 ± 1.2	40.2 ± 1.3	–
Optic chiasma $D_{1\%}$, Gy	56.0 ± 13.2	56.3 ± 11.9	55.9 ± 12.3	–
Optic nerve $D_{1\%}$, Gy	57.2 ± 13.5	57.8 ± 11.0	57.6 ± 11.7	–
Lens mean dose, Gy	5.7 ± 1.7	7.1 ± 1.5	7.1 ± 1.2	x, y
Parotid V_{30}, cm^3	56.6 ± 16.4	61.8 ± 16.7	58.0 ± 18.4	y
Monitor units	1813 ± 131	675 ± 95	759 ± 74	x, y, z

Table 4
Physical parameters representing the anatomic features averaged over the number of patients involved in group A, B1, and B2

Anatomic feature	Group A	Group B1	Group B2	$p^* < 0.05$
Shortest distance between the brain stem to PTV_{70}, cm	1.00 ± 0.10	0.74 ± 0.21	0.41 ± 0.12	I, II, III $^{(m)}$
Overlapping volume between the brain stem + 1 cm and PTV_{70}, cm^3	0.06 ± 0.12	1.19 ± 1.40	7.81 ± 4.25	II, III $^{(m)}$
Shortest distance between the brain stem to PTV_{60}, cm	0.58 ± 0.08	0.30 ± 0.09	0.23 ± 0.07	I, III $^{(a)}$
Overlapping volume between the brain stem + 1 cm and PTV_{60}, cm^3	4.99 ± 2.04	8.67 ± 2.54	19.04 ± 5.53	I, II, III $^{(m)}$
Shortest distance between the spinal cord to PTV_{70}, cm	1.25 ± 0.19	1.15 ± 0.23	1.01 ± 0.30	–$^{(a)}$
Shortest distance between the spinal cord to PTV_{60}, cm	0.76 ± 0.19	0.73 ± 0.15	0.61 ± 0.18	–$^{(a)}$
Overlapping volume between the spinal cord + 1 cm and PTV_{60}, cm^3	0.90 ± 1.63	0.76 ± 0.83	3.7 ± 2.44	–$^{(m)}$
Volume of PTV_{70}, cm^3	122.77 ± 25.34	166.08 ± 58.06	278.50 ± 83.67	I, II, III $^{(m)}$
Volume of PTV_{60}, cm^3	657.51 ± 108.23	730.63 ± 138.71	831.75 ± 150.93	III $^{(a)}$
% overlapping volume between the parotid gland and PTV_{60}, %	5.89 ± 5.37	12.2 ± 10.58	19.98 ± 16.30	III $^{(a)}$
Longitudinal distance between the lens to PTV_{60}, cm	1.13 ± 0.45	0.77 ± 0.58	0.78 ± 0.70	I, III $^{(a)}$
Shortest distance between skin to nodal target volume, cm	1.36 ± 1.33	0.50 ± 0.55	0.46 ± 0.29	I, III $^{(a)}$

ANOVA = analysis of variance.
* Statistical significance was reported between couples from either one-way ANOVA with the Tukey test (a) or Krukal-Wallis test followed by Mann-Whitney U test (m); I is group A *vs* group B1, II is group B1 *vs* group B2, and III is group A *vs* group B2.

5.1% for IMRT, RA2, and RA3, respectively. RA3 produced comparable doses to most organs as IMRT. RA2 produced inferior organ sparing in the brain stem and parotid glands. The mean dose to lens was increased by about 1.4 Gy if RA were used instead of IMRT. For this group of patients, IMRT produced better plan quality than RA.

Treatment efficiency

The average number of MU was reduced by more than 50% by using RA for all 3 groups of patients. The number of MU for RA3 was similar to that of RA2 despite of the fact that one more arc was being used.

Analysis of anatomic features and its relation with plan quality

A summary of the anatomic features of the 3 categories of patients were shown in Table 4. There was no statistically significant difference in the separation between the spinal cord and PTVs among the 3 groups of cases. The differences in percentage volume of parotid glands overlapping PTV_{60} was also insignificant between group B1 and B2. Statistically significant differences were found between all couples in only 3 of the studied features. They were the shortest distances between the brain stem and PTV_{70} ($D_{PTV70*BS}$), the overlapping volume between the brain stem with 1-cm margin and PTV_{60}, $V_{PTV60*BS}$, and the planning target volume of PTV_{70} (V_{PTV70}). They were therefore considered as the patient features to distinguish group B2 from the others. These 3 features were mainly related to the target size and its relationship with brain stem. A plot of V_{PTV70} against $D_{PTV70*BS}$ was found in Fig. 3, showing the distribution of these 2 features for all 3 groups of patients. It was observed that group B2 patients were mostly situated in the region with $D_{PTV70*BS}$ smaller than 5 mm and V_{PTV70} larger than around 200 cm^3. To show the relationship in a 3-dimensional sense, a plot of V_{PTV70} against $V_{PTV60*BS}$ was found in Fig. 4. It was observed that group B2 patients were mostly situated in the region with $V_{PTV60*BS}$ larger than around 13 cm^3 and V_{PTV70} larger than around 200 cm^3. A larger volume of PTV_{70} usually indicates a shorter distance to brain stem as indicated in Figs. 3 and 4. It was due to the fact that the target volume of NPC was usually wrapping around the brain stem in a concave shape.

In addition, the analysis in Table 4 showed that the longitudinal distances between the base of the lens and PTV_{60} for group B patients were shorter than those for group A, indicating that the superior border of the PTVs were closer to optical structures than the early cases.

Discussion

For treatments using RA, the transition between the aperture shapes from one gantry angle to the next is achieved through dynamic motion of the MLC leaves. As the gantry rotates around

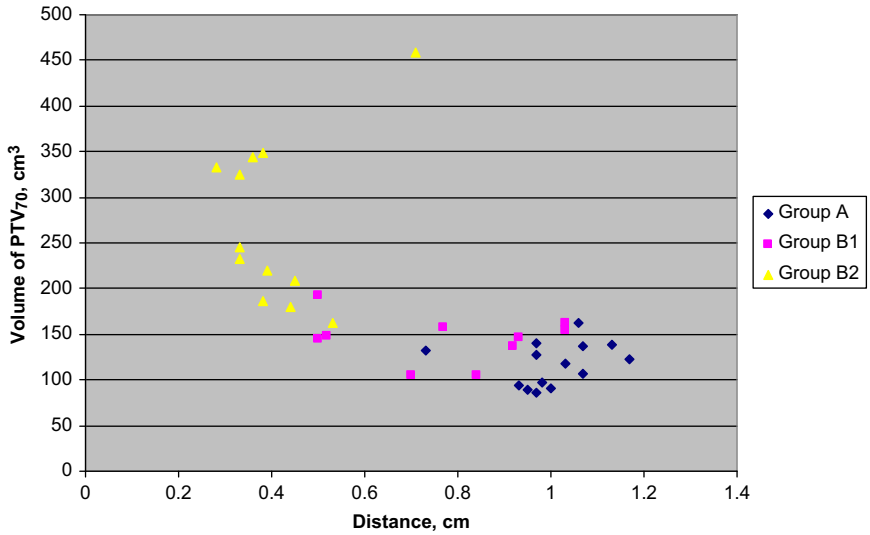

Fig. 3. Plot of the volume of PTV_{70} against the shortest distance from the brain stem to PTV_{70} for 3 groups of patients with NPC. (Color version of figure is available online.)

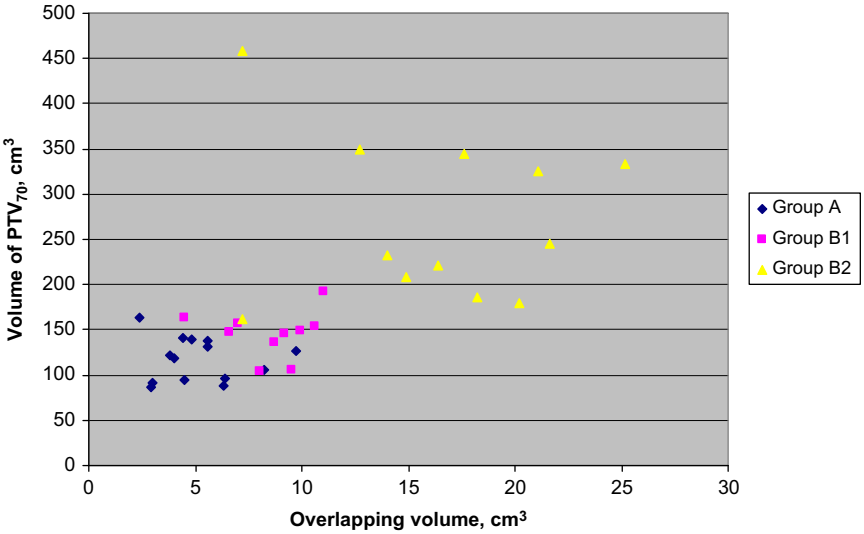

Fig. 4. Plot of volume of PTV_{70} against the overlapping volume between the brain stem and PTV_{60} the for 3 groups of patients with NPC. (Color version of figure is available online.)

the patient, the MLC leaves can only travel limited distances between subfields of adjacent beam angles. The RA delivery is constrained to a maximum leaf displacement of 0.5 cm per degree of gantry rotation.[1] As deliverability must take priority in RA treatment, an optimal field shape may have to be altered in order to produce smooth delivery. As a result, plan quality would be adversely affected for some complex cases. Although adding more arcs can provide additional freedom for beam modulation, the Eclipse planning software for RA only allows a maximum arc length of 1000°. Even if the software allows for more arc angles, adding too many arcs would further increase the treatment time and defeat the purpose of improving treatment efficiency. Those constraints to ensure smooth deliverability in RA do not apply in conventional IMRT. Static IMRT allows for more intensity modulation from specific angles to produce the optimal distribution. Our results proved that RA produced inferior plan quality for the most complex advanced NPC cases even when 3 arcs were used.

Some previous studies showed that the use of RA2 produced comparable or better plan quality compared with IMRT for head and neck cases.[8,9] Doornaert *et al.* showed that RA2 was able to produce excellent target coverage and sparing of OARs for advanced stage head and neck cases.[8] Vanetti *et al.* observed RA2 improved target coverage, target homogeneity, and sparing of the spinal cord, brain stem, and parotids compared with IMRT.[9] However, the head and neck cases involved in these studies were mainly oropharynx, hypopharynx, and larynx. Our results showed that sw-IMRT was still superior to RA2 for most NPC cases. Moreover, compared with sw-IMRT, RA3 produced superior plan quality for the early stage cases, similar plan quality for advanced cases with modest complexity, and significantly inferior target dose homogeneity for the most complex advanced NPC cases. Guckenberger *et al.* observed results that were similar to our study. They showed that for pharyngeal cancer, IMRT results were superior to double-arc VMAT, whereas triple-arc VMAT results were similar to IMRT. Another study for NPC cases performed by Lee *et al.* observed that SmartArc-based dual-arc VMAT achieved similar target coverage and slightly better homogeneity than conventional 7-field step-and-shoot IMRT.[12,13] The comparison of RA against 9-field sw-IMRT might lead to different results from that of SmartArc against 7-field step-and-shoot IMRT owing to the difference in optimization method and delivery system.

Our results suggested that the choice of replacing IMRT with RA for better plan quality depends on the complexity level of the target-organ geometry and the number of arcs used. From the anatomic analysis, it was found that for early stage NPC cases, the brain stem was around 1 cm from contoured target PTV_{70} and 5 mm or more from the PTV_{60}. On average only about 6% of the parotid glands were inside PTV_{60}. Avoiding the OARs for this category would not demand very complex intensity modulation. RA3 was able to produce similar target dose homogeneity and conformity, as well as better sparing of the spinal cord and parotid glands compared with IMRT.

For the group B2 cases, V_{PTV70} was almost twice that for the group A cases. For 10 out of the 12 cases, the PTV_{70} of the group B2 cases extend to as close as 4 mm or less to the brain stem. For the remaining 2 cases, large volume neck nodes located less than 4 mm from the skin surface were involved. To reduce the dose to the brain stem that is almost adjacent to the target, it is beneficial to have more dose modulation at specified gantry angles, especially those showing some gap between the 2 organs in the beam's eye view. For the treatment of the superficial neck nodes, it might be better to have more dose modulation for beam angles tangential to the node regions near the skin surface. More complex dose modulation at specific beam angles was less achievable using RA than IMRT. This might be the reason why IMRT can produce better plan quality than RA for this group.

Higher doses were delivered to the lens using RA when compared with IMRT. This is owing to the limitation of the collimator settings. The selected collimator angles for all the RA plans were set to be nonzero to reduce the tongue-and-groove effect. The current version of RA does not allow any optimization of the collimator angle for each arc delivery, it is impossible to exclude the lens from the jaw opening for most beam directions. For IMRT, the collimator angles could be selected for each gantry angle to exclude the lens from the jaw opening. This greatly reduces the dose because of interleaf transmission. IMRT was superior to RA if cataract was considered a clinically relevant toxicity. However, this is sometimes debatable. The ability of rotating the collimator angle during RA delivery may help in this aspect.

Conclusions

The results help the planners to identify which are the determining criteria for selecting sw-IMRT *vs* RA for NPC cases with different complexity levels. For Stage I and II NPC cases, RA3

produced better organ sparing than 9-field sw-IMRT whereas RA2 produced plan quality slightly inferior to that of sw-IMRT. For advanced stage NPC cases, whether RA can produce equivalent or inferior plan quality as sw-IMRT depends on the separation between the brain stem and the PTVs, the target sizes and the number of arcs used. In some of the advanced cases (B2), for which target sizes were very large with $V_{PTV70} > 200\ cm^3$ and $D_{PTV70*BS} < 5$ mm, sw-IMRT would be more likely to produce better target homogeneity and conformity than RA3 and RA2. For the rest of the advanced cases (B1), RA3 produced plan quality approaches to that of sw-IMRT, whereas RA2 produced inferior plan quality. For very extensive and complex target volumes such as those in the group B2, sw-IMRT is still the best choice if plan quality is the first priority unless the time of delivery is considered to be more important than plan quality.

References

1. Otto, K. Volumetric modulated arc therapy: IMRT in a single gantry arc. *Med. Phys.* **35**:310–7; 2008.
2. Yu, C.; Tang, G. Intensity-modulated arc therapy: principles, technologies and clinical implementation. *Phys. Med. Biol.* **56**:R31–54; 2011.
3. Popple, A.; Fiveash, B.; Brezovich, A.; *et al.* RapidArc radiation therapy: first year experience at the university of Alabama Birmingham. *Int. J. Radiat. Oncol. Biol. Phys.* **77**:932–41; 2010.
4. Tsai, C.L.; Wu, J.K.; Chao, H.L.; *et al.* Treatment and isometric advantages between VMAT, IMRT, and helical tomotherapy in prostate cancer. *Med. Dosim.* **36**:264–71; 2011.
5. Virekanandan, N.; Sriram, P.; Syam Kumar, S.A.; *et al.* Volmetric modulated arc radiotherapy for esophageal cancer. *Med. Dosim.* **37**:108–13; 2012.
6. Guckenberger, M.; Richter, A.; Krieger, T.; *et al.* Is a single arc sufficient in volumetric-modulated arc therapy (VMAT) for complex-shaped target volumes? *Radiother. Oncol.* **93**:259–65; 2009.
7. Verbakel, W.; Cuijpers, J.P.; Hoffmans, D.; *et al.* Volumetric intensity-modulated arc therapy vs conventional IMRT in head-and-neck cancer: a comparative planning and dosimetric study. *Int. J. Radiat. Oncol. Biol. Phys.* **74**:252–9; 2009.
8. Doornaert, P.; Verbakel, W.; Bieker, M.; *et al.* RapidArc planning and delivery in patients with locally advanced head and neck cancer undergoing chemo-radiotherapy. *Int. J. Radiat. Oncol. Biol. Phys.* **79**:429–35; 2011.
9. Vanetti, E.; Clivio, A.; Nicolini, G.; *et al.* Volumetric modulated arc radiotherapy for carcinomas of the oro-pharynx, hypo-pharynx: a treatment planning comparison with fixed field IMRT. *Radiother. Oncol.* **92**:111–7; 2009.
10. Cheung, W.K.; Lee, K.H.; Cheng, H.C.; *et al.* Comparison of RapidArc and static gantry intensity-modulated radiotherapy for nasopharyngeal carcinoma. *J. Hong. Kong. Coll. Radiol* **13**:125–32; 2010.
11. Johnston, M.; Clifford, S.; Bromley, R.; *et al.* Volumetric-modulated arc therapy in head and neck radiotherapy: a planning comparison using simultaneous integrated boost for nasopharynx and oropharynx carcinoma. *Clin. Oncol.* **23**:503–11; 2011.
12. Lee, T.F.; Ting, H.M.; Chao, P.J.; *et al.* Dual arc volumetric-modulated arc radiotherapy (VMAT) of nasopharyngeal carcinomas: a simultaneous integrated boost treatment plan comparison with intensity-modulated radiotherapies and single arc VMAT. *Clin. Oncol.* [Epub ahead of print].
13. Lee, T.F.; Chao, P.J.; Ting, H.M.; *et al.* Comparative analysis of SmartArc-based dual arc volumetric-modulated arc radiotherapy (VMAT) versus intensity-modulated radiotherapy (IMRT) for nasopharyngeal carcinoma. *J. Appl. Clin. Med. Phys.* **12**:3587; 2011.
14. International Commission on Radiation Units and Measurements, Washington, DC, 1993 report 50.
15. International Commission on Radiation Units and Measurements, Washington, DC, 1999 report 62.
16. Van't Riet, A.; Mak, A.C.; Moerland, M.A.; *et al.* A conformation number to quantify the degree of conformality in brachytherapy and external beam irradiation: application to the prostate. *Int. J. Radiat. Oncol. Biol. Phys.* **37**:731–6; 1997.
17. Wang, X.; Zhang, X.; Dong, L.; *et al.* Effectiveness of noncoplanar IMRT planning using a parallelized multiresolution beam angle optimization method for paranasal sinus carcinoma. *Int. J. Radiat. Oncol. Bio. Phys.* **63**:594–601; 2005.
18. Yartsev, S.; Chen, J.; Yu, E.; *et al.* Comparative planning evaluation of intensity-modulated radiotherapy techniques for complex lung cancer. *Radiother. Oncol.* **78**:169–76; 2006.
19. Wu, B.; Ricchetti, F.; Sanguineti, G. Patient geometry-driven information retrieval for IMRT treatment plan. *Med. Phys.* **36**:5497–505; 2009.